Vol. 154: 7–14, 2023
https://doi.org/10.3354/dao03735

DISEASES OF AQUATIC ORGANISMS
Dis Aquat Org

Published June 1

Myxobolus lentisuturalis infection in a farmed population of goldfish *Carassius auratus* from the USA

Caitlin M. Hepps Keeney[1,*], Thomas B. Waltzek[2], Pedro H. de Oliveira Viadanna[2], Salvatore Frasca Jr.[3], Emily Reinhardt[3], Jan Lovy[4], Gregory A. Lewbart[1]

[1]Department of Clinical Sciences, North Carolina State University College of Veterinary Medicine, Raleigh, NC 27607, USA
[2]Department of Infectious Diseases and Pathology, University of Florida College of Veterinary Medicine, Bldg #1379, Mowry Road, Gainesville, FL 32610, USA
[3]Department of Pathobiology and Veterinary Science, University of Connecticut, 61 North Eagleville Road, Unit 3089, Storrs, CT 06269, USA
[4]New Jersey Department of Environmental Protection, Fish & Wildlife, Office of Fish & Wildlife Health & Forensics, 605 Pequest Rd, Oxford, NJ 07863, USA

ABSTRACT: *Myxobolus lentisuturalis* is a myxozoan parasite of piscine muscle that has been described in goldfish *Carassius auratus* and Prussian carp *Carassius gibelio*. This report documents a naturally occurring infection of *M. lentisuturalis* in a population of farmed goldfish in the USA. Postmortem examination was performed on 4 affected goldfish. Gross findings included large cystic cavities along the dorsal midline filled with caseous exudate. Histopathology revealed myxozoan plasmodia and spores in the epaxial muscles with varying degrees of granulomatous and necrotizing myositis accompanied by lymphohistiocytic meningoencephalitis. Spore morphology and dimensions were consistent with *M. lentisuturalis*, as observed by light microscopy. PCR and sequence analysis of the small subunit ribosomal DNA of infected muscle samples from 2 goldfish confirmed the parasite to have 99–100% nucleotide identity to *M. lentisuturalis* sequences recovered from similar cases of this parasite infecting goldfish in China and Italy and Prussian carp in China. This is the first reported case of *M. lentisuturalis* in the USA and furthers the understanding of the pathogenicity of this under-described parasite.

KEY WORDS: *Myxobolus lentisuturalis* · Goldfish · *Carassius auratus* · Myxozoan · Myositis

1. INTRODUCTION

Goldfish *Carassius auratus* are a popular ornamental cyprinid fish that are traded in more than 100 countries (Trujillo-González et al. 2018). Although the species originated in China, the ornamental fish trade has expanded their range globally (Trujillo-González et al. 2018). Continued import and trade increases the risk for introduction of novel pathogens, including parasites. Parasites have been detected infecting imported goldfish in more than 14 countries, a number which will likely expand as globalization progresses (Trujillo-González et al. 2018).

The Myxozoa are metazoan parasites of both vertebrates and invertebrates (Frasca et al. 2018). Several myxozoan species are of economic and ecological importance in fish, with the most notable being *Myxobolus cerebralis*, the causative agent of whirling disease (Wolf & Markiw 1984, Lom & Dyková 2006, Gruhl 2015, Frasca et al. 2018). *M. lentisuturalis* is a little-known myxozoan parasite that infects

*Corresponding author: cmheppsk@ncsu.edu

Publisher: Inter-Research · www.int-res.com

piscine skeletal muscle and was first described in 2002 as a parasite of Prussian carp *C. gibelio* in China (Dyková et al. 2002). Dyková et al. (2002) described the parasite's tropism for muscle in these Prussian carp and identified its invertebrate oligochaete host *Branchiura sowerbyi*, a developmental similarity to *M. cerebralis* that uses *Tubifex tubifex* as its invertebrate host (Wolf & Markiw 1984, Zendt & Bergersen 2000, Hallett et al. 2006).

A 2009 report from Italy described *M. lentisuturalis* infection in goldfish *C. auratus*, expanding the understanding of the parasite's life cycle to include a raabeia-type actinospore within the oligochaete host and demonstrating that spore development alternates between an invertebrate and vertebrate host (Caffara et al. 2009). The report also described the characteristic dorsolateral humps of the epaxial muscles seen with this disease and the histologic features associated with infection (Caffara et al. 2009). A recent study from Chongqing, China, described an infection of the biliary tract of a goldfish with *M. lentisuturalis*, without associated clinical disease (Wang et al. 2019). Despite the difference in anatomic site of infection, samples exhibited no genetic difference (Wang et al. 2019). Host and environmental factors that could influence the pathogenicity and tropism of this myxozoan are not known.

Outside of these reports, a paucity of information exists regarding *M. lentisuturalis*, despite the potential economic implications for goldfish aquaculturalists. Although this parasite has not been associated with significant mortality, the deforming lesions preclude the sale of affected goldfish and could lead to long-term outbreaks and morbidity within a given stock. The geographic distribution and pathogenicity of this parasite have yet to be fully elucidated, and it has not previously been reported outside of China and Italy. This study describes the first reported outbreak of *M. lentisuturalis* in a population of farmed goldfish in the USA. Morphologic and molecular analysis of this parasite and histologic description of the infection within the goldfish host are provided.

2. MATERIALS AND METHODS

2.1. Animals

From 2019 to 2020, a commercial goldfish farm in North Carolina, USA, suffered an outbreak of cavitating muscular lesions that were expansile, occasionally ulcerative, and located on the dorsal midline just caudal to the head (Fig. 1). The goldfish farm is composed of outdoor mud ponds with a local river as the water source. All goldfish were bred onsite, and 12–15 ponds were spawned yearly. Although the farm was not observed by the authors, according to correspondence with the farm manager, approximately 80% of the ponds were impacted, with 20–40% of the individuals in each pond affected. Lesions were not visible on fry but became apparent once goldfish reached approximately 5 cm in length. No mortalities were reported in association with these lesions. No new fish were added to the system prior to the outbreak; all fish were spawned on the premises. Fish were fed a commercial diet consisting of 34% crude protein, 4% crude fat, 6% crude fiber, and 8% phosphorous. Water quality was tested 4–5 times yearly, and no major concerns were noted. The farm reported an average pH of 7.0, ammonia of 0.2 mg l^{-1}, nitrite of 0.02 mg l^{-1}, and a temperature range of 14.5–21°C (58–70°F). Additional details of

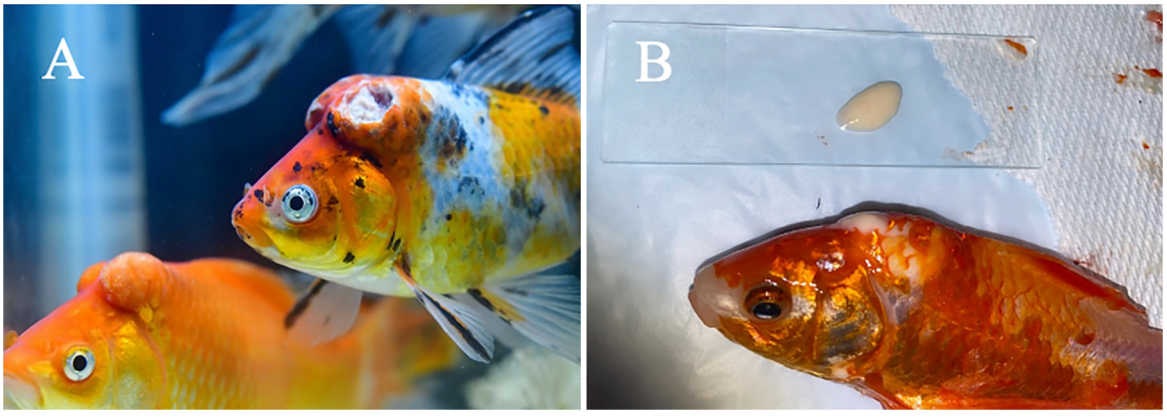

Fig. 1. Gross lesions of *Myxobolus lentisuturalis* infection in goldfish *Carassius auratus.* (A) On both sides of dorsal midline immediately caudal to the head were expansile, bilobulated, ovoid subcutaneous lesions, one with ulceration of the overlying skin. (B) The contents consisted of abundant viscous, pale tan, opaque exudate

the farm are withheld to protect the anonymity of the business.

2.2. Necropsy

Four goldfish with cavitating muscular lesions were euthanized and postmortem examinations were performed. Affected musculature from 2 goldfish were collected and frozen at −80°C until they were processed for DNA extraction as described below. Cavitating muscular lesions from a single fish were also collected and fixed in Karnovsky's fixative to evaluate spore morphology in wet mounts. Formalin-fixed tissue samples were trimmed to represent gross lesions, routinely processed for embedment in paraffin, and sectioned at a thickness of 4 µm. The following tissues were examined on hematoxylin-and-eosin- and Wolbach Giemsa-stained slides: skin, skeletal muscle, cartilage, bone, spinal cord, brain, kidney, interrenal organ, intestine, gallbladder, mesentery, pancreas, heart, gill, spleen, swim bladder, testis, and ectopic thyroid (kidney). Selected tissues were stained with Twort's Tissue Gram, Ziehl-Neelsen, and Luna stains for further evaluation of the histomorphologic features of the myxozoan (Luna 1968, Lillie & Conn 1977, Sheehan & Hrapchak 1987). Histologic sections were photographed with an Olympus BX60 microscope and DP27 digital camera. Wet mounts of myxospores fixed in Karnovsky's fixative were examined using differential interference contrast (DIC) microscopy using a Zeiss Axioplan 2 research microscope. Images were taken with a microscope-mounted digital camera (Gryphax Arktur, Jenoptik). Digital images were taken with samples under a 100× oil immersion objective, and spore measurements were taken directly from digital images using the ProgRes CapturePro software version 2.10.01.

2.3. Genetic sequencing

The frozen muscle samples from 2 goldfish were processed for DNA extraction using a DNeasy Blood and Tissue Kit (Qiagen) according to the manufacturer's instructions. The DNA extracts were amplified by PCR with the primer pairs ACT1r and Myxgen4f that generate overlapping fragments of approximately 1000 and 1200 bp, respectively, to obtain the complete small subunit ribosomal DNA (ssu rDNA) sequence (Barta et al. 1997, Hallett & Diamant 2001, Diamant et al. 2004). Reaction volumes were 30 µl and consisted of 0.15 µl of Platinum *Taq* DNA Polymerase (Invitrogen), 3.0 µl of 10× PCR buffer, 1.2 µl of 50 mM $MgCl_2$, 0.6 µl of 10 mM dNTPs, 1.5 µl of 20 µM forward and reverse primers, 17.6 µl of molecular grade water, and 4.5 µl of DNA template for a total of 100 ng. An initial denaturation step of 94°C for 5 min was followed by 36 cycles of a 94°C denaturation step, a 55°C annealing step, and a 72°C extension step, each step run for 1 min, and a final extension step at 72°C for 5 min. PCR products were subjected to electrophoresis in a 1% agarose gel stained with ethidium bromide. Amplicons of the expected size were purified using a QIAquick PCR Purification Kit (Qiagen). The concentration of purified amplicons was determined fluorometrically using a Qubit 3.0 Fluorometer and dsDNA BR Assay Kit (Life Technologies) before submitting for Sanger sequencing. Purified DNA was sequenced in both directions using the primers described above on an ABI 3130 platform (Applied Biosystems). The sequence data were assembled and edited in CLC Genomics Workbench 7.5 software (Qiagen). Primer sequences and regions of low-confidence base calling were excluded at both the 5′ and 3′ sequence ends. BLASTN analysis was performed using the edited and assembled sequences (https://blast.ncbi.nlm.nih.gov/).

3. RESULTS

All fish with visible lesions were culled. Affected ponds were not drained, and no method of disinfection was implemented. The outbreak clinically resolved after culling affected individuals, and no new lesions have been noted over the ensuing 2 yr. Postmortem examination of the 4 clinically affected fish revealed a large cystic cavity filled with heterophilic exudate along the dorsal midline. No other abnormalities were noted.

Histologic examination revealed myxozoan developmental stages, including plasmodia and spores, in the epaxial skeletal muscle of all 4 goldfish and in the skin of 3. Myxozoan plasmodia and spores replaced extensive regions of muscle, accompanied by necrotic myofibers and varying degrees of inflammation (Fig. 2A). In 2 goldfish, myxozoan spores were present within large, occasionally coalescing granulomas within affected muscle (Fig. 2B). In specimens where lesions within muscle extended into the dermis, myxozoan developmental stages were associated with chronic dermatitis, foci of epidermal erosion and ulceration, hemorrhage, and

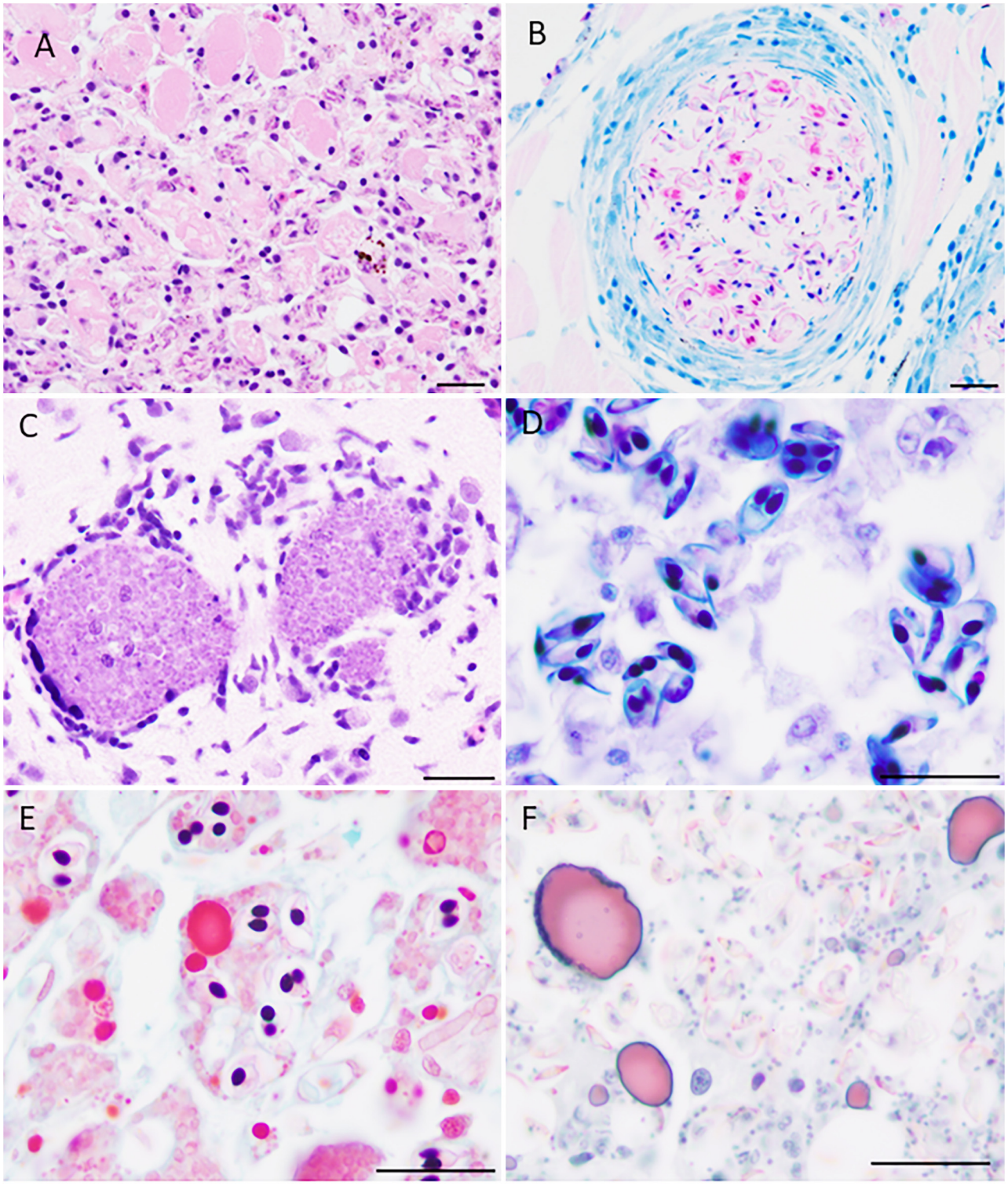

Fig. 2. Developing stages of *Myxobolus lentisuturalis* in tissue section from goldfish *Carassius auratus*. (A) Myxozoan plasmodia and spores replace muscle with degeneration and necrosis of myofibers. H&E. (B) A granuloma within skeletal muscle containing myxozoan spores. The valve cells are variably acid-fast while polar capsules stain blue. Ziehl-Neelsen. (C) Non-sporogonic myxozoan plasmodia with an attendant lymphohistiocytic encephalitis in the neuroparenchyma. H&E. (D) The valve cells of myxospores are stained light blue while pyriform polar capsules are stained deep blue. Wolbach Giemsa. (E) Polar capsules of myxozoan spores are Gram-positive. Twort's Tissue Gram stain. (F) Valve cells of myxospores are stained red. Luna. All scale bars = 20 µm

in one goldfish, myxozoan spores were present within the epidermis. In the brain and spinal cord, plasmodia were present in the endomeninges and neuroparenchyma, in some instances accompanied by lymphohistiocytic meningoencephalitis (Fig. 2C). Sporogonic stages were not identified in the brain; however, both plasmodia and spores were present within the foci of myelomeningitis in one goldfish. The internal polar capsules of myxospores stained blue with Wolbach Giemsa (Fig. 2D), were Gram-positive (Fig. 2E), and blue with the Ziehl-Neelsen stain (Fig. 2B). To ensure that extensive areas of myositis did not have an intercurrent microsporidian infection (a principal concern given the sites of infection and the fish host), a Luna and Gram stain were applied, both of which are known to selectively stain microsporidial spores in tissue sections (Peterson et al. 2011). Myxozoan valve cells were stained but other cells within sporogonic and non-sporogonic plasmodia in the skeletal muscle and central nervous system were not, and no microsporidian spores were observed (Fig. 2F). Granulomas were also seen in various organs of some individuals, including the kidney (2 of 4), spleen (2 of 4), heart (1 of 4), and liver (1 of 4), and these did not have evidence of myxospores. Branchial lamellar epithelial hyperplasia with lamellar fusion was seen in 2 cases, with one case having rare monogeneans.

DIC microscopy revealed large numbers of fully developed myxospores consistent in morphology to *Myxobolus* species (Fig. 3A). The myxospores from specimens preserved in Karnovsky's fixative were ellipsoidal, measuring 11.4 ± 0.4 µm (range: 10.4–12.5 µm) by 7.1 ± 0.4 µm (range: 6.4–8 µm) in frontal view (n = 50). Previously reported ranges of *M. lentisuturalis* spore dimensions were 11.8 µm (range: 11.2–12.4 µm) by 7.6 µm (range: 7.2–8.4 µm) and 10.5 µm (range: 9.0–11.0 ± 0.6 µm) by 6.6 µm (range: 6.0–7.0 ± 0.4 µm) (Dyková et al. 2002, Caffara et al. 2009). Pyriform-shaped polar capsules were of equal size, measuring 4 ± 0.2 µm (range: 3.5–4.5 µm) by 2.6 ± 0.2 µm (range: 2.2–3 µm) (n = 50). Previously reported ranges of *M. lentisuturalis* polar capsules were 3.7 µm (range: 3.0–4.5 ± 0.4 µm) by 2.2 µm (range: 2.0–3.0 ± 0.3 µm) and 4.2 µm (range: 4.0–4.4 µm) by 2.5 µm (range: 2.0–2.8 µm) (Dyková et al. 2002, Caffara et al. 2009). The majority of polar capsules had 4 coils in the polar tubule (n = 48), though 2 polar capsules had 5 coils. The polar capsules were situated in the anterior part of the myxospores and ended slightly over the middle part of the spores, and the sporoplasm comprised the posterior portion of the spore (Fig. 3A,B). The long axis of the polar capsules was roughly parallel with the long axis of the myxospores. In sutural view, the thickness of spores was 4.7 ± 0.4 µm (range: 3.9–5.5 µm) (n = 50) and the sutural ridge was not apparent (Fig. 3C). PCR yielded fragments of the expected sizes. The 2 assembled overlapping ssu rDNA sequences were identical and 1977 bp in length after regions of low-confidence base calling were excluded. BLASTN analysis revealed 100% nucleotide identity and 100% coverage to *M. lentisuturalis* (AY278563), previously characterized from Italian pond-reared goldfish that displayed identical cavitating muscular lesions (Caffara et al. 2009). The next top-scoring BLASTN hit (99.85% identity and 100% coverage) was to *M. lentisuturalis* characterized from Prussian carp caught in Lake Bao'an in China (Dyková et al. 2002). The *M. lentisuturalis* sequence generated in this study has been submitted to GenBank (OP374272).

A second spore type, most consistent in morphology to a *Henneguya* species, was rarely detected in the wet mounts of the cavitating muscular lesions (Fig. 3D). These relatively smaller myxospores were pyriform in shape and contained 2 caudal projections of the valves on the posterior portion of the spore. The main spore body measured 7.7 ± 1.0 µm (range: 6.6–8.6 µm) by 5.2 ± 1.1 µm (range: 4.0–6.4 µm) (n = 3). The caudal appendages of the spores measured between 6 and 15 µm in length, though it is possible that these were not complete, as these structures are fragile and prone to breaking during processing.

4. DISCUSSION

This report documents the occurrence and resolution of an outbreak of *Myxobolus lentisuturalis* in a commercial goldfish farm. Communications with the farmers since the outbreak have indicated that culling the visibly affected goldfish was a successful management strategy. Previous research indicates that infection of the goldfish host occurs through an intermediate oligochaete host, *Branchiura sowerbyi*, and not through direct transmission (Dyková et al. 2002, Caffara et al. 2009). Although we did not attempt to identify oligochaetes from the mud of ponds harboring affected goldfish in our study, *B. sowerbyi* or a similar oligochaete remains the most likely source of infection in this outbreak (El-Matbouli & Hoffmann 1989, 1993, El-Mansy et al. 1998). Therefore, culling alone was unlikely to have been the only factor in preventing ongoing infection, though it may have reduced the number of spores released back into affected ponds (Lom & Dyková

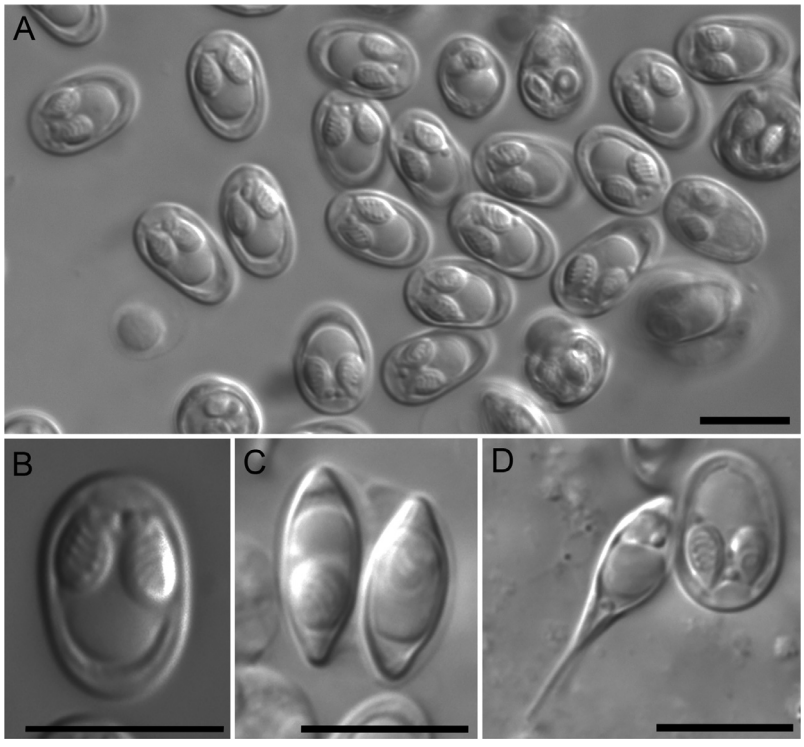

Fig. 3. Myxospores from goldfish *Carassius auratus* as seen under differential interference contrast microscopy. (A) Mature myxospores consistent in morphology to *Myxobolus lentisuturalis.* (B) Frontal view of *M. lentisuturalis* with polar capsules taking up slightly more than the anterior half of the spores. (C) Side view of *M. lentisuturalis* myxospores with an apparent lack of a sutural ridge. (D) *Henneguya*-like myxospore adjacent to *M. lentisuturalis*. All scale bars = 10 µm

2006). We postulate that oligochaetes contained within the mud of the local river that supplied the ponds were the most likely source of infection since all goldfish were bred onsite. Environmental factors such as temperature and the introduction of fresh river water into the ponds likely contributed to the resolution of clinical signs, in addition to culling affected individuals (Aston 1968). It cannot be ruled out that infected oligochaetes may still be present within the mud layer of the ponds, potentially causing a recurrence of lesions in the future (Aston 1968). Due to privacy concerns from the goldfish farmers, further investigation was not pursued.

DIC light microscopy confirmed that the morphology of myxospores herein was consistent with the original morphological description of *M. lentisuturalis* (Dyková et al. 2002). The spore and polar capsule dimensions, apparent absence of a sutural ridge, and presence of 4 coils to the polar filament, all observed here, are morphological features that distinguish *M. lentisuturalis* (Dyková et al. 2002, Caffara et al. 2009). Previous reports of this parasite examined fresh spores, while spores in our study were fixed in Karnovsky's fixative, which can affect spore dimensions. Nevertheless, the measurements of fixed spore dimensions in this report were within the ranges of those previously published for fresh spores (Dyková et al. 2002, Caffara et al. 2009). Though the predominant lesions were associated with *M. lentisuturalis*, the rare finding of myxospores more consistent with a *Henneguya*-like species may indicate that co-infections occurred with at least one other myxozoan. *Henneguya* species are closely related to *Myxobolus* and are known to infect many fish species with varying pathogenicity (Lom & Dyková 2006, Carriero et al. 2013). One of the 4 goldfish submitted for necropsy had spores that were morphologically distinct from those of *M. lentisuturalis* in the skeletal muscle, further supporting a possible co-infection. A second possibility is that these morphologically distinct spores represent aberrant *M. lentisuturalis* spores. Although it has not yet been reported in this species, other *Myxobolus* species have been documented to produce aberrant spores with caudal projections that could mimic the appearance of a *Henneguya* species (Liu et al. 2010, 2019). Without further molecular analysis, however, it is not possible to distinguish between these 2 possibilities (Eszterbauer et al. 2006).

Histopathologic examination of affected goldfish revealed myositis and meningoencephalomyelitis caused by *M. lentisuturalis* plasmodia and spores. The lesion in muscle is consistent with the initial report of *M. lentisuturalis* in Prussian carp, which described a similar myositis but did not report invasion into the spinal cord (Dyková et al. 2002). The finding of myositis and meningoencephalomyelitis is comparable to the report from Italy describing *M. lentisuturalis* in goldfish, which documented myositis and invasion of spinal nerves but did not examine central nervous tissue (Caffara et al. 2009). One of the 4 goldfish had plasmodia in its bile ducts. In that goldfish, plasmodia were luminal, found in low numbers, and were not associated with cholangitis or cholecystitis. While this is similar to the report documenting asymptomatic

M. lentisuturalis infection in the gallbladder of a goldfish (Wang et al. 2019), this could also represent infection by a third myxozoan. Nevertheless, asymptomatic infection of the gallbladder likely represents an intercurrent infection of lesser clinical significance. The results from the goldfish in this study provide further evidence that infection of muscle and nervous tissue is the typical presentation of cyprinid species infected with *M. lentisuturalis*.

M. lentisuturalis is an uncommonly reported piscine parasite, with previous infections being reported in China and Italy. This is the first reported case of *M. lentisuturalis* in the USA and furthers the understanding of its pathogenicity. Although no mortalities have been documented secondary to *M. lentisuturalis*, long-term or recurring infection within a farmed population could lead to significant economic losses due to the deforming nature of the parasite. Additionally, asymptomatic goldfish that are sold into the ornamental fish trade have the potential to infect other environments, other fish, and to propagate the spread of the parasite. Fish on this farm were all bred onsite, though the original source of breeding fish was not revealed by the owners. As the international ornamental fish trade continues to grow, the potential for spread of *M. lentisuturalis* throughout the USA and internationally is of increasing concern. Culling affected individuals appears to have been an effective management strategy, though long-term monitoring of outbreaks and documentation of possible recurrences will be crucial in mitigating outbreak severity and economic losses associated with this parasite.

Acknowledgements. The authors thank Dr. Tatiane Terumi Negrão Watanabe and Dr. Monica Caffara for their correspondence and input on study design.

LITERATURE CITED

Aston RJ (1968) The effect of temperature on the life cycle, growth and fecundity of *Branchiura sowerbyi* (Oligochaeta: Tubificidae). J Zool 154:29–40

Barta JR, Martin DS, Liberator PA, Dashkevicz M and others (1997) Phylogenetic relationships among eight *Eimeria* species infecting domestic fowl inferred using complete small subunit ribosomal DNA sequences. J Parasitol 83: 262–271

Caffara M, Raimondi E, Florio D, Marcer F, Quaglio F, Fioravanti ML (2009) The life cycle of *Myxobolus lentisuturalis* (Myxozoa: Myxobolidae), from goldfish (*Carassius auratus auratus*), involves a raabeia-type actinospore. Folia Parasitol 56:6–12

Carriero MM, Adriano EA, Silva MRM, Ceccarelli PS, Maia AAM (2013) Molecular phylogeny of the *Myxobolus* and *Henneguya* genera with several new South American species. PLOS ONE 8:e73713

Diamant A, Whipps CM, Kent ML (2004) A new species of *Sphaeromyxa* (Myxosporea: Sphaeromyxina: Sphaeromyxidae) in devil firefish, *Pterois miles* (Scorpaenidae), from the northern Red Sea: morphology, ultrastructure, and phylogeny. J Parasitol 90:1434–1442

Dyková I, Fiala I, Nie P (2002) *Myxobolus lentisuturalis* sp. n. (Myxozoa: Myxobolidae), a new muscle-infecting species from the Prussian carp, *Carassius gibelio* from China. Folia Parasitol 49:253–258

El-Mansy A, Molnar K, Szekely C (1998) Development of *Myxobolus portucalensis* Saraiva & Molnár, 1990 (Myxosporea: Myxobolidae) in the oligochaete *Tubifex tubifex* (Müller). Syst Parasitol 41:95–103

El-Matbouli M, Hoffmann RW (1989) Experimental transmission of two *Myxobolus* spp. developing bisporogeny via tubificid worm. Parasitol Res 75:461–464

El-Matbouli M, Hoffmann RW (1993) *Myxobolus carassii* Klokaceva, 1914 also requires an oligochaete, *Tubifex tubifex*, as intermediate host in its life cycle. Bull Eur Assoc Fish Pathol 13:189–192

Eszterbauer E, Marton S, Racz OZ, Letenye M, Molnar K (2006) Morphological and genetic differences among actinosporean stages of fish-parasitic myxosporeans (Myxozoa): difficulties of species identification. Syst Parasitol 65:97–114

Frasca S Jr, Wolf JC, Kinsel MJ, Camus AC, Lombardini ED (2018) Osteichthyes. In: Terio KA, McAloose JS (eds) Pathology of wildlife and zoo animals. Elselvier, San Diego, CA, p 953–993

Gruhl A (2015) Myxozoa. In: Wanninger A (ed) Evolutionary developmental biology of invertebrates, Vol 1. Springer-Verlag, Wien, p 165–177

Hallett SL, Diamant A (2001) Ultrastructure and small-subunit ribosomal DNA sequence of *Henneguya lesteri* n.sp. (Myxosporea), a parasite of sand whiting *Sillago analis* (Sillaginidae) from the coast of Queensland, Australia. Dis Aquat Org 46:197–212

Hallett SL, Atkinson SD, Erséus C, El-Matbouli M (2006) Myxozoan parasites disseminated via oligochaete worms as live food for aquarium fishes: descriptions of aurantiactinomyxon and raabeia actinospore types. Dis Aquat Org 69:213–225

Lillie RD, Conn HJ (1977) HJ Conn's biological stains: a handbook on the nature and uses of the dyes employed in the biological laboratory, 9th edn. Williams & Wilkins, Baltimore, MD

Liu Y, Whipps CM, Gu ZM, Zeng LB (2010) *Myxobolus turpisrotundus* (Myxosporea: Bivalvulida) spores with caudal appendages: investigating the validity of the genus *Henneguya* with morphological and molecular evidence. Parasitol Res 107:699–706

Liu Y, Lövy A, Gu Z, Fiala I (2019) Phylogeny of Myxobolidae (Myxozoa) and the evolution of myxospore appendages in the *Myxobolus* clade. Int J Parasitol 49: 523–530

Lom J, Dyková I (2006) Myxozoan genera: definition and notes on taxonomy, life-cycle terminology and pathogenic species. Folia Parasitol 53:1–36

Luna LG (1968) Manual of histologic staining methods of the Armed Forces Institute of Pathology, 3rd edn. McGraw Hill, New York, NY

Peterson TS, Spitsbergen JM, Feist SW, Kent ML (2011) Luna stain, an improved selective stain for detection of microsporidian spores in histologic sections. Dis Aquat Org 95:175–180

Sheehan DC, Hrapchak BB (1987) Theory and practice of histotechnology, 2nd edn. Battelle Press, Columbus, OH

Trujillo-González A, Becker JA, Jutson KS (2018) Parasite dispersal from the ornamental goldfish trade. Adv Parasitol 100:239–281

Wang M, Zhao Y, Yang C (2019) The impacts of geographic and host species isolation on population divergence of *Myxobolus lentisuturalis.* Parasitol Res 118:1061–1066

Wolf K, Markiw ME (1984) Biology contravenes taxonomy in the Myxozoa: new discoveries show alternation of invertebrate and vertebrate hosts. Science 225:1449–1452

Zendt JS, Bergersen EP (2000) Distribution and abundance of the aquatic oligochaete host *Tubifex tubifex* for the salmonid whirling disease parasite *Myxobolus cerebralis* in the upper Colorado River basin. N Am J Fish Manage 20:502–512

Editorial responsibility: Michael Kent, Corvallis, Oregon, USA
Reviewed by: S. Atkinson and 1 anonymous referee

Submitted: September 9, 2022
Accepted: December 8, 2022
Proofs received from author(s): May 26, 2023